PHOTOINDUCED IRREVERSIBLE EFFECTS ON MAGNETIC PROPERTIES AND ALLIED PHENOMENA IN MAGNETIC OXIDES XI

K. Hisatake, I. Matsubara, and K .Maeda,
Department of Physics, Kanagawa, Dental College,Kanagawa 238-0003, Japan
S.Abe,
Dept. of Electrical Engineering Kanagawa University, Yokohama 221-8686, Japan
S. Kainuma,
Ashikaga Institute of Technology, Tochigi 326-8558, Japan
Carlos de Francisco, Jose Maria Munoz, Oscar Alejos, Pablo Hernandez, Carlos Torres
Dpto. Electricidad y Electronica, Facultad de Ciencias Universidad de Valladolid,
Valladolid, E-47071 Spain

Abstract- A review is presented of the various experimental results that have thus far been developed for the study of disaccommodation(DA) in a single crystals of yttrium iron garnet in 1998, which is irradiated with laser (the most effective wavelength is 700 nm) or white light at 77 K. Then, a remarkable change of the temperature dependence of complex permeabilities and is observed, which is specific to photoinduced magnetic effect. Simultaneously, conspicuous double peaks of DA around 125 K and 250 K below room temperature were found to be induced by light-irradiation, with correlative onset of the irreversible decrease of permeability sensitive to demagnetization at low temperature. Furthermore, photoinduced Accommodation is observed in this sample at comparatively high frequency for the first time. In addition, three peaks of (DA) in polycrystalline CaVIn-garnet have been for the first time observed , double peaks. in order to explain these observations, we propose that oxygen defects provide a mechanism for occurrence of photomagnetic effects and discussion of its validity; the review of these area of our laboratories in 1998 is given. On the basis of these results a model for the photoinduced magnetic after effects of YIG is proposed and discussed.

1. Introduction

1.1 Phenomenological aspect of magnetic after effects

First, we present a theoretical study of frequency-dependent dynamics of domain walls in magnetically ordered materials when magnetic aftereffects (MAE'S) appear. By MAE is meant a delayed change in magnetization accompanying a change in the magnetic field[1]. We exclude from this definition the magnetization delays made by eddy currents and structural changes or aging of the substance. Snoek[2] explained the nature of this phenomenon by means of a model consisting in a ball placed on a curved concrete surface covered with a mud layer of a finite thickness. From a phenomenological point of view, after the ball is displaced to a new position, it will sink into the layer of mud gradually, changing its equilibrium position. On the other hand, if we forced the ball to oscillate back and forth around the minimum position of the concrete surface (ac magnetization), we would find three possible situations. If the viscosity of mud is increased at low temperatures, the ball will move on the hardened surface of the mud with very low loss. In a similar way, if the viscosity is

decreased at high temperatures, the ball will move through the unviscous layer of mud. At the intermediate temperatures, the motion of the ball is must severely damped, resulting in very large loss. Neel [3] modified Snoek's concept of magnetic after effect(MAE) in certain respects, including detailed calculations. He introduced the idea that MAE's have their origin in the relaxation of the induced magnetic anisotropy due to a redistribution of magnetic dipoles into the lattice. The induced anisotropy does not differ from the magneto-crystalline anisotropy as far as their origin is concerned but, being related to local anisotropy arrangements in the lattice, it usually exhibits lower symmetry than that of the crystal as a whole[4]. Hence, MAE's happen to be very useful for basic research, because such studies yield information about lattice symmetry and dynamics[5]. In accordance with the model proposed by Neel, we have considered that the motion of a Bloch wall under the influence of an applied magnetic field is then defined by the sum of different stresses: the applied magnetic field stress, an elastic term, a damping term, and a stress connected with MAE'S. We have written the corresponding wall dynamics equation by means of such stresses and we have solved it using harmonic fields. As an important result, we have obtained that wall motion amplitude is a function of time that can both increase or decrease depending on the applied field frequency. Finally, we have verified this behavior experimentally for a polycrystalline yttrium-iron-garnet YIG sample by means of the so-called magnetic disaccommodation (DA)technique.

1.2 Theoretical Aspects of MAE'S

The motion of a Bloch wall under the influence of an applied magnetic field, possibly time dependent, is defined by the sum of different stresses. To the applied magnetic. field stress, we must add an elastic term that refers the wall to its equilibrium position and connected with lattice internal stresses, dislocations, etc., another one, proportional to its speed, to take account of damping effects that prevent a free wall oscillation when it changes its position, and finally, a stress due to the redistribution of magnetic dipoles within the lattice. Hence, we write the following dynamic equation[3] for the Bloch wall(see the appendix I),

$$\ddot{u} + v\dot{u} = \vec{H}(t)(\vec{M}_2 - \vec{M}_1) + P(u,t), \qquad (1.1)$$

u being the wall instantaneous position. m the wall inertial mass, v the damping coefficient. - $R(u)$ an elastic term, and M_1 and M_2 the magnetization on each side of the wall. The redistribution stress $P(u,t)$ is obtained by computing the instantaneous anisotropy energy associated to a unity surface of the wall considering the lattice symmetry and the directions of the magnetization M_1 and M_2. This stress can be written as[6].

$$P(u,t) = - Po \left\{ \int_0^t f[u(t') - u(t)] g(t - t') dt' + o(u) \left[1 - \int_0^t g(t') dt'\right] \right\}. \quad (1.2)$$

The first term in the sum takes account of the wall evolution and is connected with magnetic aftereffects in the material. It refers the wall to all of its previous positions, but weighted by the function $g(t)$. This function is defined by

$$g(t) = \int_0^x p(\tau)/\tau^{-t/\tau} d\tau,$$

$p(\tau)$ being the probability of relaxation process of time constant, and it is strictly decreasing. As can be expected, the stress due to the immediately preceding positions is the most important in the weighting. On the other hand, $f(U)$ depends on the wall type.[4] For example, in j the case of a 90° wall of thickness d, it was found that

$$f_{90}(U) = -\left(\frac{U}{d} + \coth\frac{U}{d} - \frac{U}{d}\coth^2\frac{U}{d}\right). \quad (1.3)$$

On the other hand, the second term in $P(u,t)$ takes into account the magnetic viscosity. As the $-R(u)$ term in Eq. (1.1), it is a stress that refers the wall to its last equilibrium position. However, its effect vanishes for large t. The function $o(u)$ gives the strength of this stress and depends on the initial state of the lattice. This function can be defined as $o(u)=[u(0)-u]$, $u(0)$ being the wall initial position, when the material is initially in a steady state. But, if the material is in a demagnetized state, that is, when the directions of the magnetic dipoles inside the material are equally distributed, $o(u) \equiv 0$. Taking up again Snoek's model, the first situation corresponds to the case in which the ball would be totally sunk in the mud. In the second one, the mud would be uniformly distributed over the concrete. This last case allows us to study in detail the magnetic induced anisotropy relaxation and, then, the aftereffect phenomena in these materials. Hence, we consider the demagnetized state as the initial state in our study. To simplify the solution of Eq. (1.1),it is usually considered that the wall motion stays in the zone where the $-R(u)$ function is approximately linear. On the other hand, the magnetic field stress can be written as proportional to its modulus and to the saturation magnetization,

$$m\ddot{u} + v\dot{u} = -ru + \gamma H(t) Ms - P(u,t). \cdots\cdots (1.4)$$

Some authors[7] have proposed solutions to this equation by means of an attraction between the wall and some mobile elements called pinning centers that is used instead of the $P(u,t)$ stress. In this work, we will consider that wall displacements are also in the linear zone of the $f(U)$ function, with the same idea that we have given above for the elastic term, that is, $f(U) = -fU$, where f is now a constant, and

$$m\ddot{u} + v\dot{u} = -ru + \gamma H(t) M_s - fP_0\left[\begin{matrix} u(t')G(t) \\ -\int_0^t u(t')g(t-t')dt' \end{matrix}\right]. \cdots\cdots (1.5)$$

Here, we have introduced the relaxing function

$$G(t) = \int_0^t g(t')dt' = 1 - \int_0^\infty e^{-t/\tau} p(\tau)d\tau. \cdots\cdots (1.6)$$

This function increases from $G(0)$ to $G(\infty)=1$. In a simple case, $G(t)$ presents multi-exponential features, but it depends on the applied model for the relaxation. In some cases, a description of this relaxation in terms of the so-called stretched exponential[8] has been found useful to describe some experimental results of magnetic after effects in magnetite samples.[9]

A. Low-frequency motion

When the applied magnetic field has very low frequency, we can suppose that the inertial and damping terms in Eq. (1.5) are negligible. Hence, Eq. (1.5) is no longer a differential equation and

$$0 = -ru + \gamma H(t) M_s - fP_0 \left[u(t')G(t) - \int_0^t u(t')g(t-t')dt' \right] \cdots\cdots (1.7)$$

The solution of this equation can be found if the wall is characterized by a single time constant and the field is harmonic, that is, $H(t) = H_0 \sin \omega t$, resulting in

$$u(t) = u_0 e^{-t/\tau(1+\eta)} \Big/ [1 + \eta(1 - e^{-t/\tau})]^{1/(1+\eta)}$$

$$\times \int_0^t e^{t'\tau(1+\eta)(1/\tau * \sin\omega t' + \omega \cos\omega t')} \Big/ [1 + \eta(1 - e^{-t'/\tau})]^{\eta/(1+\eta)} dt'$$

$$\cdots\cdots (1.8)$$

where we have introduced the parameters $u_0 = \gamma MsHo/r$ and $\eta = fP_0/r$. The first one represents the maximum wall amplitude in the absence of induced anisotropy relaxation, and the value defines the ratio between the elastic constant r and another elastic term added by the induced anisotropy relaxation term. When $\eta \ll 1$, this second term prevails. Depending on the $\omega\tau$ product we will consider three different situations. First, the wall response for a constant frequency is given by the inverse of the time constant τ, that is, $\omega\tau = 1$, taking the η value as a parameter. So, relaxation and wall motion occur at the same speed. We can see that the wall motion is damped by the magnetic induced anisotropy relaxation and also, how the wall motion and the applied field are out of

phase as η value increases. In all cases, the displacements tend to remain near the wall equilibrium position. On the other hand, when $\omega\,\tau \gg 1$, the redistribution of the magnetic dipoles is fast enough to keep the system in equilibrium. Hence, we can propose the following approximate response:

$$\int_0^t u(\theta)g(t-\theta)d\vartheta \qquad (1.9)$$

As the frequency increases, the redistribution effect will modulate the wall motion, modifying its speed. Then, the frequency spectrum of the wall response *u(t)* spreads slightly, especially near the field frequency ω. On the other hand, if the time constants of the redistribution are greatly above the inverse of the field frequency, the $g(t\text{-}0)$ acts as a low-pass filter in the convolution term and, hence, this term vanishes. In this third case, an approximate solution of Eq. (1.7) is given by ,

$$u(t) \approx \frac{\gamma M_s}{\gamma[1+\eta G(t)]} H(t). \cdots\cdots (1.10)$$

Wall response under the action of a harmonic magnetic field with a frequency given by the time constant inverse is sufficiently high to take account of the induced anisotropy relaxation phenomena. We can see that both approximate responses, Eqs (1.9) and (1.10), are in good agreement with the exact solutions. Wall response under the action of a harmonic magnetic field.

B. High-frequency motion.

Using the same approximation, as in obtaining Eq. (1.10), we can rewrite Eq. (1.11) for a high-frequency magnetic field $H(t) = H_O \sin\omega t$ as

$$\ddot{u} + 2\omega_n \dot{u} + \omega_n^2[1+\eta G(t)]u = u_0\omega_n^2 \sin\omega t, \cdots\cdots (1.11)$$

being $\omega_n = \sqrt{r/m}$ the wall natural resonance frequency and δ the damping coefficient. This differential where equation can be solved numerically. The results are obtained for two illustrative cases. In the first one, we find that the wall amplitude increased one, we can see how the amplitude increases initially with time, passes through the maximum and dynamics, on term will increase with time, modifying the elastic term increasing in the same way as the wall resonance frequency that is

$$\omega_0 = \omega_n\sqrt{1+\eta G(t)}, \cdots\cdots (1.12)$$

The transient caused by this change will vanish if it is sufficiently slow. The wall response is thus approximated by

$$u(t) \approx \frac{u_0}{\sqrt{\left[1-\frac{\omega^2}{\omega_n^2}+\eta G(t)\right]^2+4\delta^2\frac{\omega^2}{\omega_n^2}}}\sin[\omega t-\varphi(t)], \tag{1.13}$$

where

$$\tan\varphi(t)=\frac{2\delta\frac{\omega}{\omega_n}}{1-\frac{\omega^2}{\omega_n^2}+\eta G(t)} \cdots\cdots (1.14)$$

Transient will vanish if for a given δ value, we have

$$\delta\omega_n >> \frac{\eta}{\tau_m}$$

if $0<\delta \leqq 1$, (1.15)

$$\left(\delta-\sqrt{\delta^2-1}\right)\omega_n >> \frac{\eta}{\tau_m}$$

otherwise, (1.16)

where τ_m is the lowest relaxation time constant. Dumping effects are found to decrease with time. Depending on the field frequency , the wall amplitude will wither decrease, increase, or both with rime. According to our theory, in a demagnetized sample of a magnetic ordered material under the influence of an applied magnetic ordered material under the influence of an applied magnetic field, the motion amplitude of Bloch walls varies with time depending on the field frequency.

On the other hand, photoinduced magnetic effect is a very interesting problem, related to magnetic after effect and potential for an application in photo-memory and evaluation of vacancy-type defects of materials. These effects can be divided into the I-effect (Si~0.1mol doped YIG) and the II-effect (Si~0.01mol doped YIG)[10], depending on whether is dominant or not the polarization state of light for the observation. The origin of I-effect was explained as a redistribution of uniaxial anisotropy of Fe^{2+} along one of the four cubic directions of octahedral sites, while the II-effect was attributed to the different behaviors of Fe^{2+} close to and far from Si^{4+} ions. On the other hand, the induced preferred directions within the domain wall in soft materials create localized potential minima. As these minima become deeper with time, the mobility of the domain wall will decrease. The gradual decrease of μ_i' after demagnetization or magnetic slow relaxation of μ_i' is called the disaccommodation (DA)[11]. In this report, we present the observation of photoinduced DA in not Si- but Ca-doped YIG and a clue to explain why it is possible for the single or double peaks of

photoinduced DA to exist in YIG single crystal. A remarkable photoinduced disaccommodation (DA) of magnetic permeability μ' is observed in yttrium iron garnet (YIG) single crystal with very low contents of Ca: these double peaks of DA are around 125 K(0.46eV) and 200 K (0.60 eV) with correlative onset of the irreversible decrease of μ' insensitive to demagnetization at lower temperature than 250K. In addition, we observed the lowest temperature peak of DA is strongly frequency dependent and at 1 kHz it is cancelled by the accommodation (A) phenomenon. For these observations, we propose that the pinning center may be due to a photoinduced structure change around oxygen defects. Transients will vanish where $\omega \tau$ represents the lowest relaxation time constant. Dumping effects are found to decrease with time. It is expected that depending on the field frequency, the wall amplitude will either decrease, increase, or both with time.

III. Experimental

According to our theory, in a demagnetized sample of a magnetic ordered material under the influence of an applied magnetic field, the motion amplitude of Bloch walls varies with time depending on the field frequency. We have verified this behavior experimentally. We have evaluated wall mobility by measuring reversible magnetic permeability. As a first approximation, the magnetization in the material can be considered as proportional to domain-wall displacements. The high purity samples of YIG were fablicated from a floating zone method, except for intentional dopants Ga^{3+}:0.0625 replaced by Fe^{3+} and Ca^{2+}:0.001 by Y^{3+} which is expected to increase the penetration depth of light. In the sample, however, a considerable oxygen vacancy is incorporated of the order of 0.001mol estimated from spectroscopic method. In this experiment, two samples (A) and (B) are used, both of which have 4 mm in the outer diameter and 2 mm in the inner diameter cut from the same ingot of YIG single crystal. Source of irradiating the samples was visible light from a xenon lamp, since no conspicuous differences of the characteristics among the many other kinds of light sources, but the most effectiveness in these phenomena is the light wavelength of about 1μm. The measurements of photoinduced irreversible decrease of the real part of permeability, $\mu'(t,T)$, photoinduced DA and or usual DA in the dark were carried out, using an automated equipment which allows one to measure the time dependence of $\mu'(t_1,T)$, at various temperatures T with any arbitrary time intervals $\Delta t = (t_2 - t_1)$ after demagnetization. The experimental results could be represented relaxation curves of the magnitude of $\Delta R / \mu'(t_1,T)$, where $\Delta R = \mu'(t_1, T) - \mu'(t_2, T)$. Here, t_1 =2sec and $t_2 = 2^n$ (n=2,3,--,7) sec for a sample (A)and t_1 =5sec and t_2 =50 sec for a sample (B) after demagnetization (see the appendix I).

IV. Experimental results and discussion

4.1. Photoinduced irreversible decrease of μ' (PID)

First, we observed the photoinduced irreversible decrease of μ' (termed as PID) in these samples (A) and (B). The effect in the sample (A) in Fig.1 is not due to DA, since it cannot be returned buck to the original state before irradiation or being insensitive to demagnetization (not shown in the figure). This shows the light intensity dependence of PID in YIG (sample A). Measuring frequency is 140 Hz. It is natural to observe for the response time to become reduced with the light intensity. Next, measuring field intensity and frequency dependence of the PID were studied and are shown in Fig.2 and Fig.3, respectively. In general, the spectrum of μ' of YIG is characterized by two distinct regions of dispersion. The lower one less than 100 kHz results from the relaxation of domain wall contribution, while the dispersion at higher than 100MHz is due to the magnetic resonance in an effective field by anisotropy and internal demagnetizing fields[12].

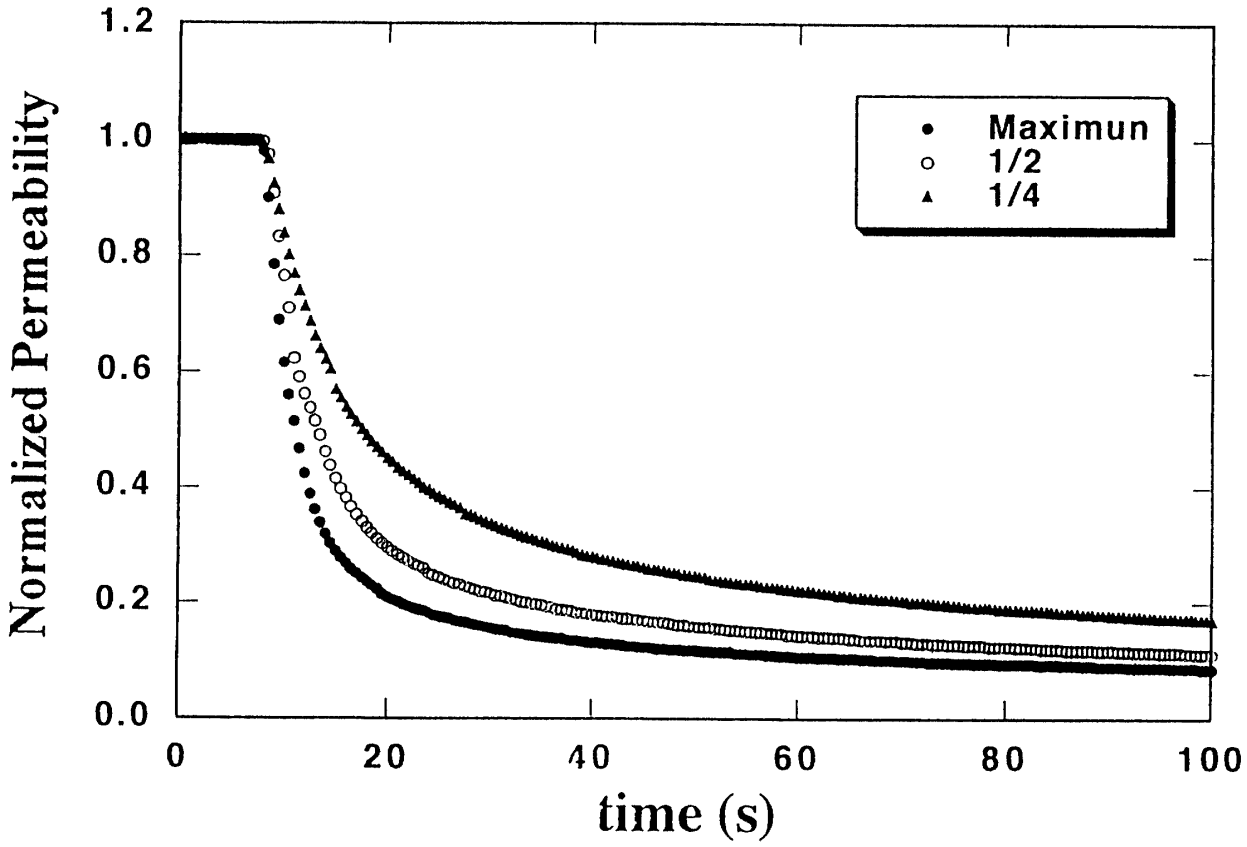

Fig.1 Time dependence of photoinduced irreversible decrease in permeability μ' (PID) in YIG (sampleA). Measuring field and frequency are 3mOe and 140Hz, respectively.

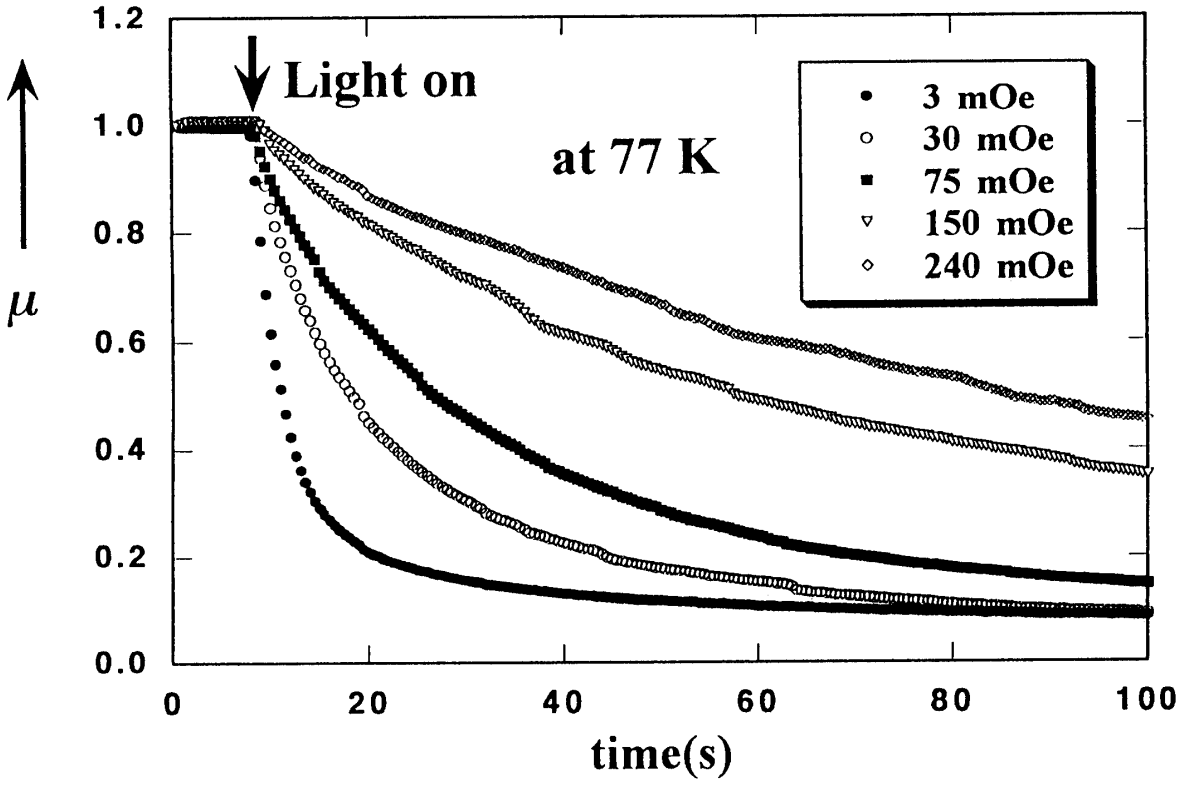

Fig.2 Time dependence of the permeability μ' (PID) as a function of magnetic field in YIG. (sample A). Measuring frequency is140 Hz.

In our experiments taking into consideration of the strong frequency dependent PDA, the low frequency region must be, furthermore divided into the regions lower and higher than 1 kHz .

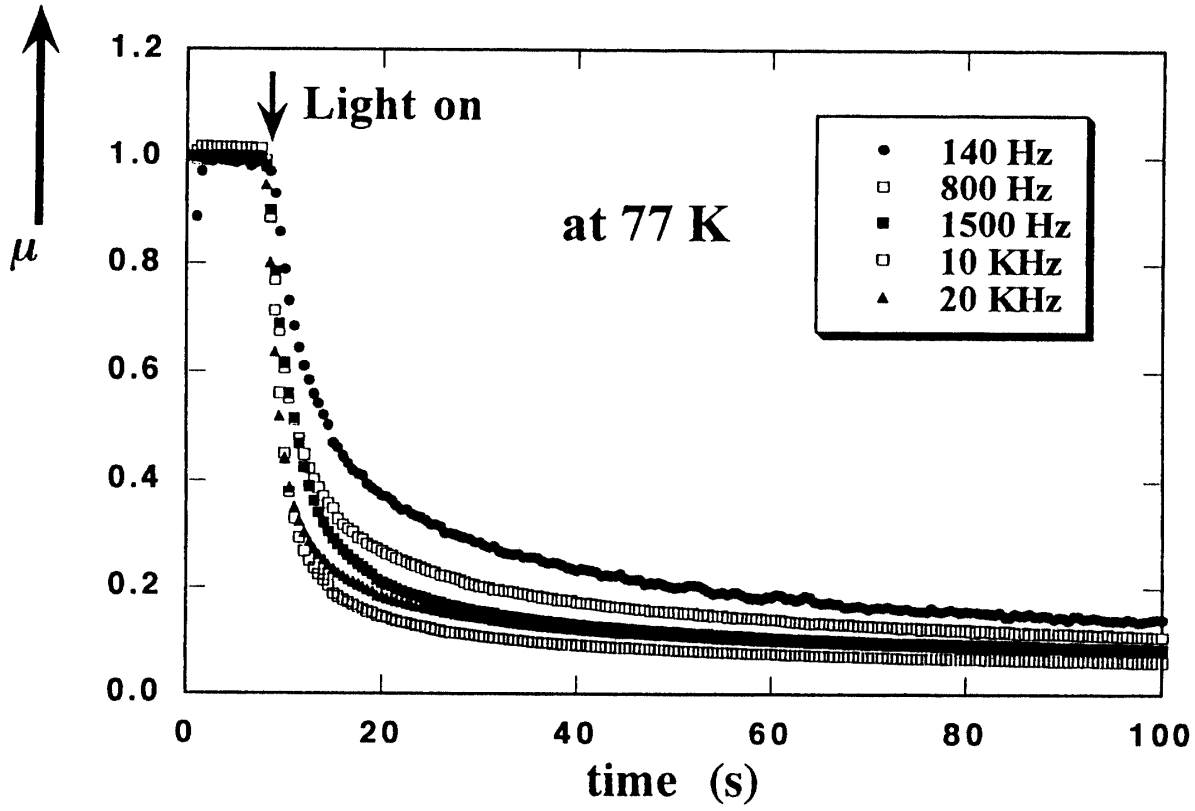

Fig.3 Time dependence of photoinduced irreversible decrease in permeability μ' (PID) in YIG (sam ple A). Measuring field is 3mOe.

An explanation for PID has been mentioned in the introduction. But it is possible that another model could exist in our previous paper[13] : photoinduced atomic rearrangements or charge change around vacancy triggered by an electronic excitation in the crystals, within a domain wall may lead to the formation of a stabilization potential acting as pinning center. Photoinduced migration is known in the F-center of an ionic crystal, where self-trapped excitons mediate such a process[14]. These processes can be represented by a configurational coordinate diagram such as that shown in Fig.4. Although the diagram is schematic, the features essential to PID are present, especially the metastability at low temperature in a distorted configuration.

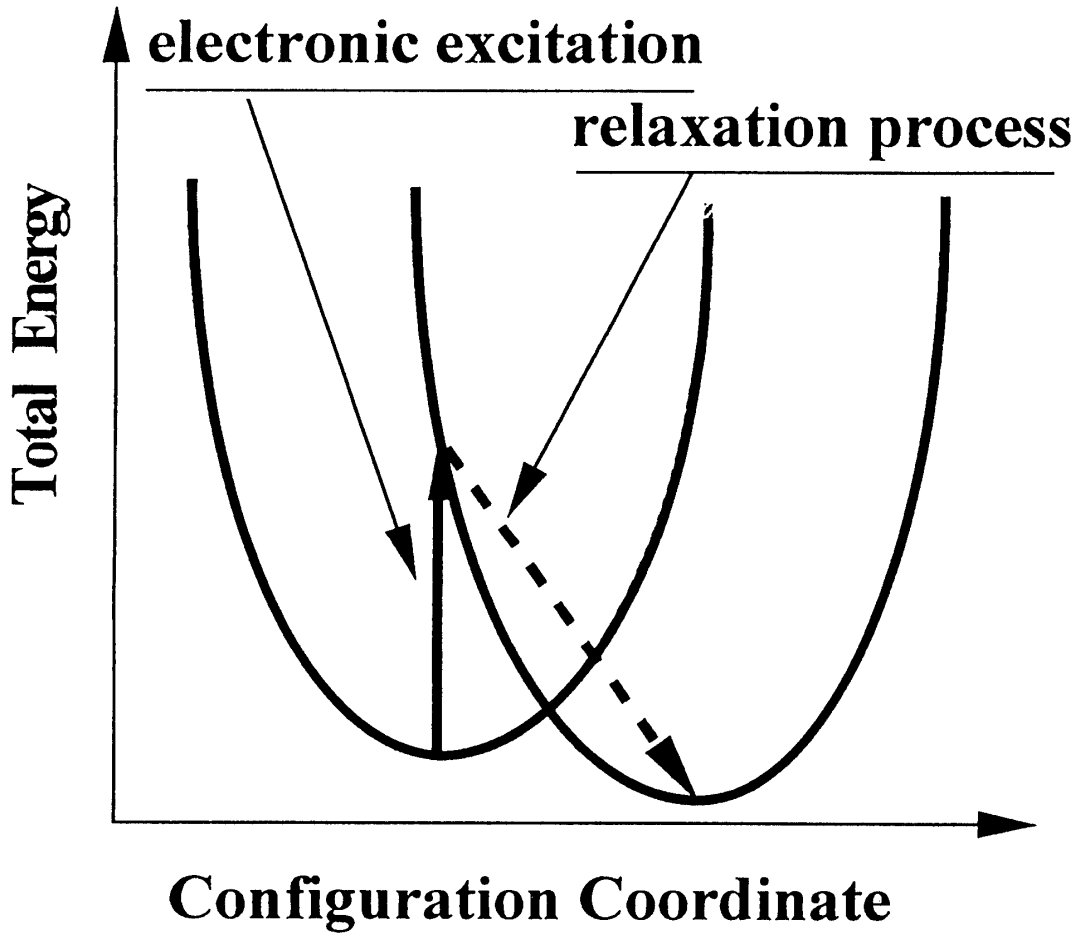

Fig.4 Configurational coordinate diagram for the explanation of photoinduced decrease of μ'(PID).

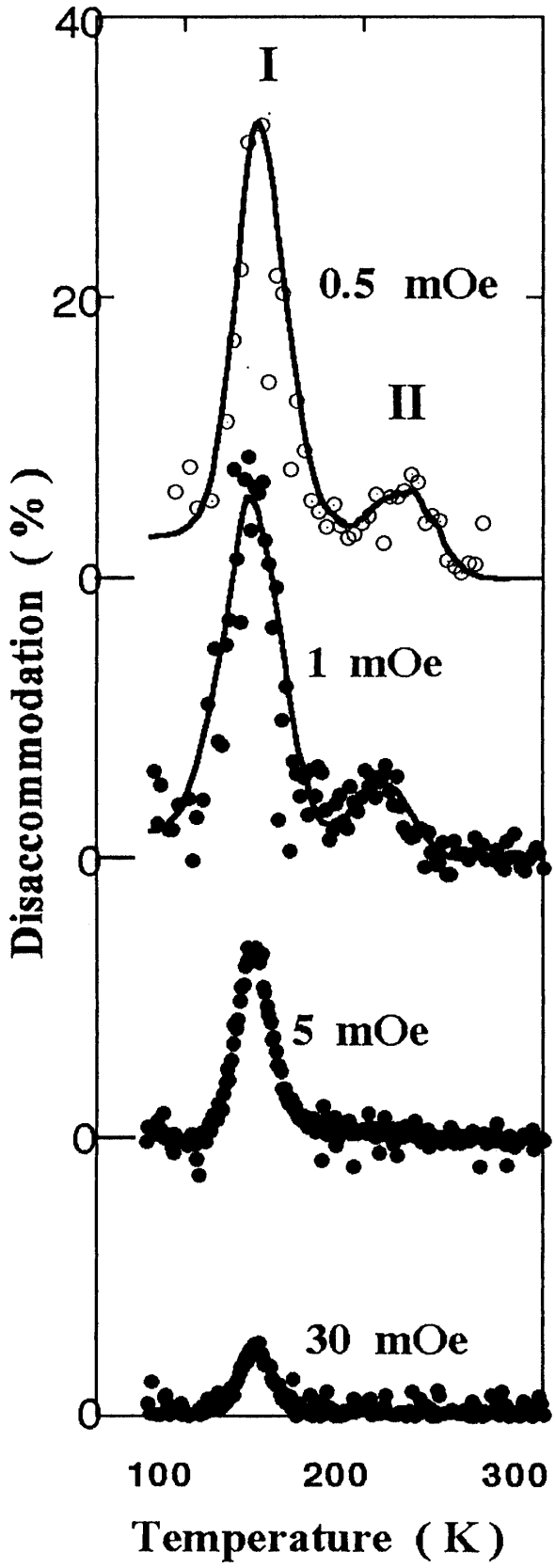

Fig.6 Magnetic field variation of the photoinduced DA (PDA) *vs* temperature of YIG (sample B). Measuring frequency is 0.14 kHz.

In addition, we observed the third peak (DAIII, 0.88 eV) around the room temperature, independent of irradiation around the room temperature in some samples. The peak shows strongly the sample-dependence although the peak is perfectly reproducible for a given sample. An explanation for a PDA is also presented, including a migration of oxygen vacancy, since some kinds of carriers such as electron and vacancy must themselves to form an induced anisotropy and stabilize the magnetic domain wall so that the total energy takes the minimum. In a previous paper[15], we proposed that DAI is due to a time dependent induced anisotropy from a translation of oxygen vacancy V_o without trapped electron, DAII is from V_o with one trapped electron and DAIII is V_o with trapped two electrons, taking into consideration of the mobility of V_o. This explanation is ,however, not unique but the alternatives are numerous[16].

4.3 Photoinduced accommodation in YIG

Figure 7 shows the three dimensional plots of the frequency dependence of PDA in sample (B). It should be noted that the height of DA I is reduced; at 560 Hz DAI disappears completely and at 1 kHz negative DAI, that is accommodation(A) grows with the measuring frequency. Figure 8 shows the two dimensional representation of the similar results in the sample (A). In some samples, photoinduced DA cannot be observed[see Appendix II] , but one of us (K.H) would like to advice to reexamine if it could be masked by the accommodation.

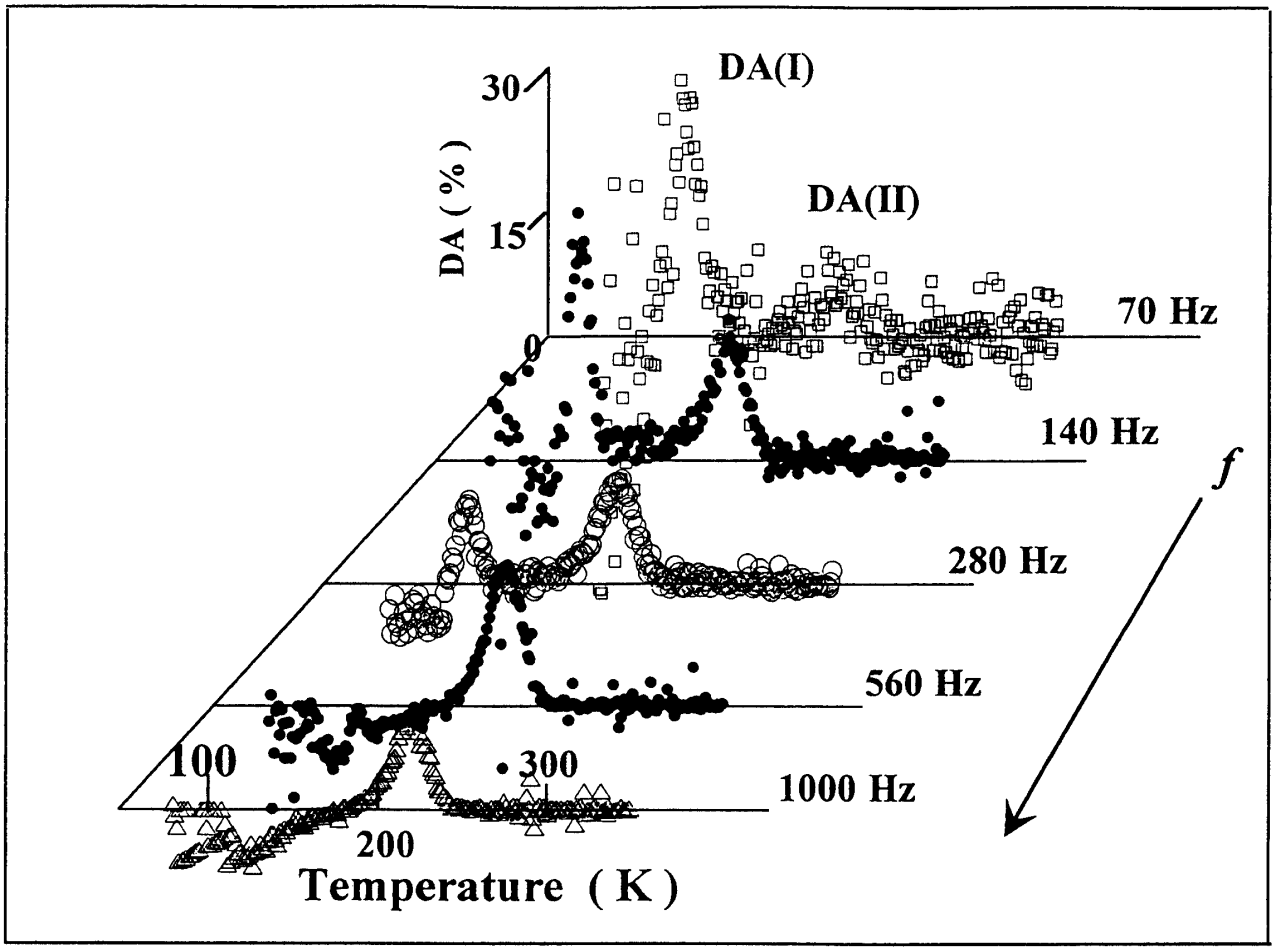

Photoinduced DA vs temperature vs frequency

Fig.7 Three dimensional plots of the photoinduced DA(PDA) vs temperature vs frequency in the sample (B).

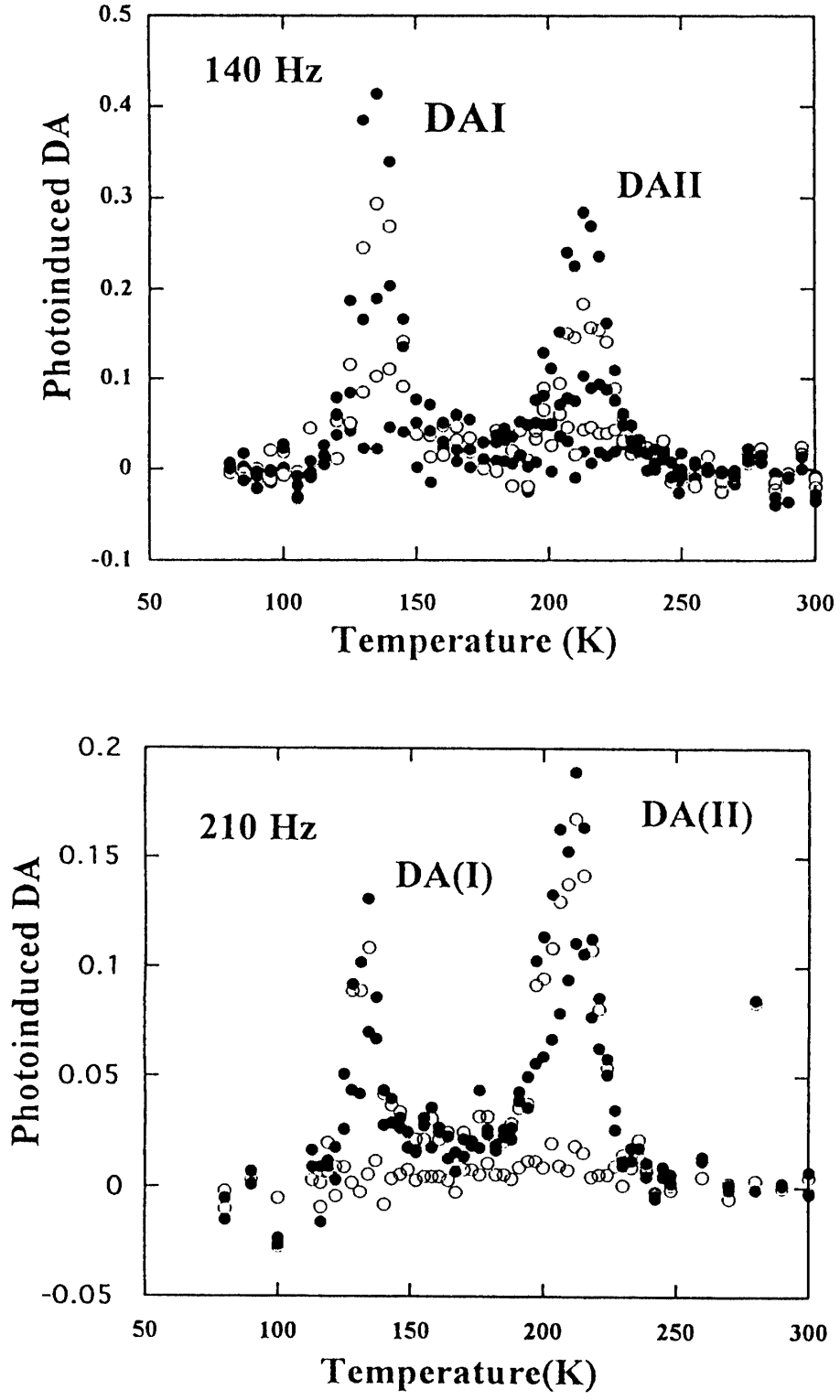

Fig 8 Two dimensional plots of the photoinduced DA(PDA) vs temperature vs frequency (lower frequency) in the sample(A).

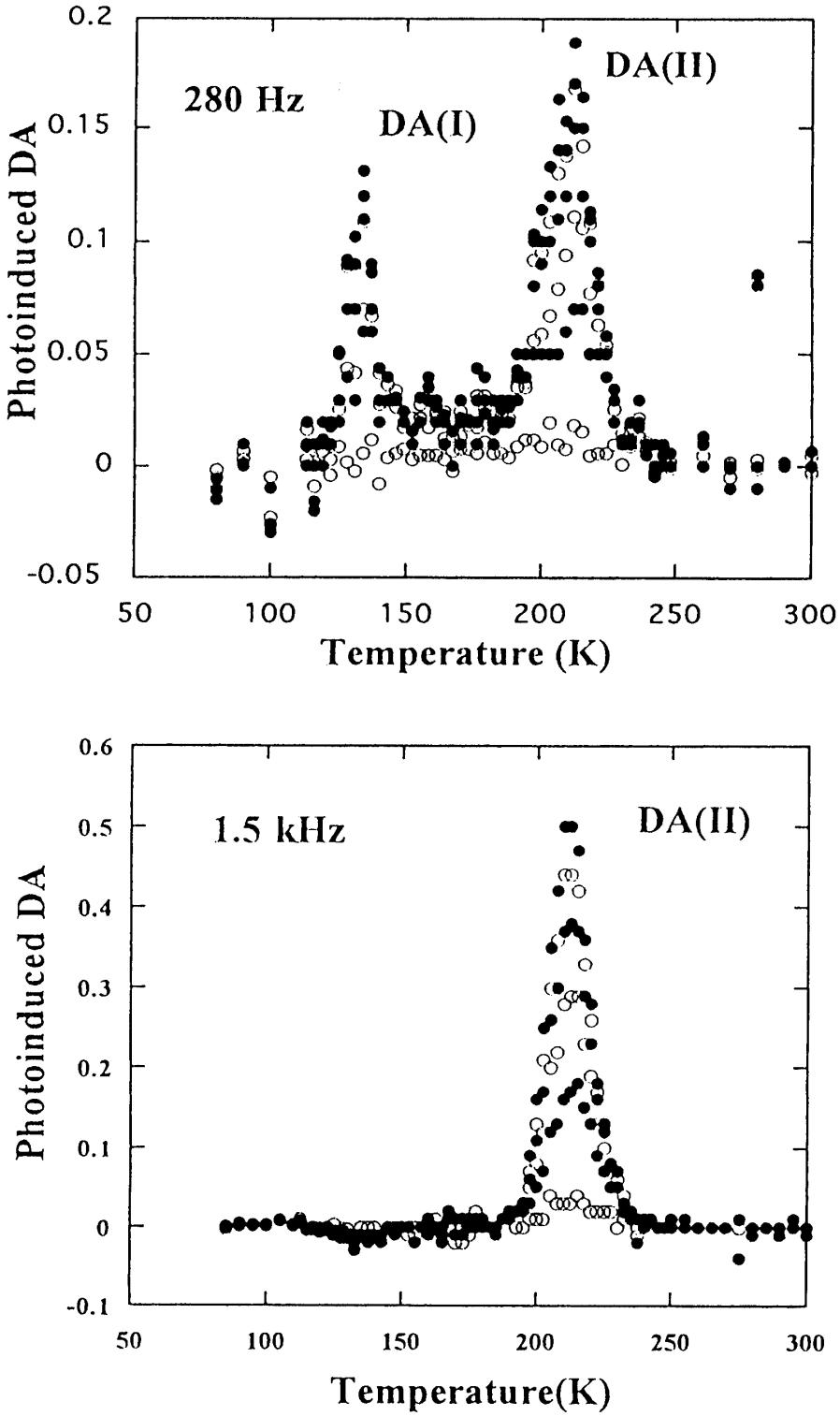

Fig.8-contined. Two dimensional plots of the photoinduced DA(PDA) vs temperature vs frequency(higher frequency) in the sample (A).

4.4 Band Structure of YIG

When studying the band structure of YIG, one encounters the difficult problems as in other transition metal oxides like, e.g., NiO. The problems are caused by the presence of the d-levels, which may form more or less localized bands. As in normal semiconductors there also are broad band-like states, namely a valence band which mainly is derived from oxygen 2p-orbitals and a conduction band derived from iron 4s-states or yttrium 5s-states. The energy gap between these broad bands is generally large in the transition metal oxides. From optical reflection measurements on YIG, Galuza et al. (18) showed the presence of very strong bands with absorption coefficients as high as 9×10^5 cm^{-1} at 10.5 and 18.2 eV. The presence of a band near 10 eV with a high oscillator strength is confirmed by an analysis of the dispersion curves of a number of garnets [19]. The high value of the absorption coefficient agrees with dipole allowed p -> s transitions. At energies below 10 eV charge transfer transitions with smaller oscillator strengths are observed. As mentioned in section 111 (the energetically lowest lying band is situated at 2.81-2.88 eV)[20 , 21]. In view of the high Faraday rotation and the low oscillator strength, Wittekoek et al. [21] attributed this band to the parity forbidden transition between oxygen 2p-states and iron 3d-states mainly octahedral in character. At 3.35 eV another charge .transfer transition is found and be-cause of its very low Faraday rotation and the high oscillator strength this band is assigned for symmetry allowed transition from O(2p) ↑Fe(3d) states mainly tetrahedral in character. However, the possibility of Fe-Fe charge transfer cannot be excluded [22]. From a derivative of the absorption. spectrum, Wemple et al. [23] and Blazey [24] find an extra band at 3.16 eV which they also attribute to a charge transfer transition. The high temperature conduction measurements gave a value of 2.85 eV (or a value smaller than 3.16 eV) for the energy gap[25]. This value agrees with the energy of the lowest charge transfer band. We therefore assume that the states involved in the optical transition can be identified with the valence and conduction band states. This identification implies that the n-type conduction takes place in a narrow band derived from Fe(3d)-orbitals mainly octahedral in character. If the degree of localization is high, occupied states in this band may be denoted as Fe^{2+} states. Let us now consider our model further in connection with the experimental results. The half width of the charge transfer absorption band at 2.88 eV is about 0.3 eV, i.e., more than 10 times kT. This means that at least one of the two levels involved in this transition has to be broad. Fontana and Epstein [26] interpreted their measurements of a temperature independent Hall mobility in Si-doped YIG (n-type) in terms of band conduction. The activation energy of 0.3 eV should in this case be the ionization energy of the charge carriers from the Si ions. On the other hand, Elwell and Dixon [27] interpreted the observed temperature independence of the Seebeck coefficient in Hf-doped YIG in terms of the hopping model. In this case the activation energy of the conductivity is ascribed to the activation energy of the drift mobility solely. From previous investigations by the present authors on polycrystalline n-type YIG there is evidence that , the temperature dependence of the conductivity in these samples is mainly due to an ionization of the charge carriers [28]. The activation energy was rather high, 0.56~0.9 eV, and these experiments therefore do not exclude a small activation energy of the mobility. Also for p-type samples the conduction mechanism is uncertain. For Ca or Pb doped YIG one finds an activation energy of 0.35-0.40 eV near room temperature. However, from the absorption spectrum ofYIG with a lead excess more information is obtained. This absorption is due to transitions from

the valence band to the Pb acceptor level [29].

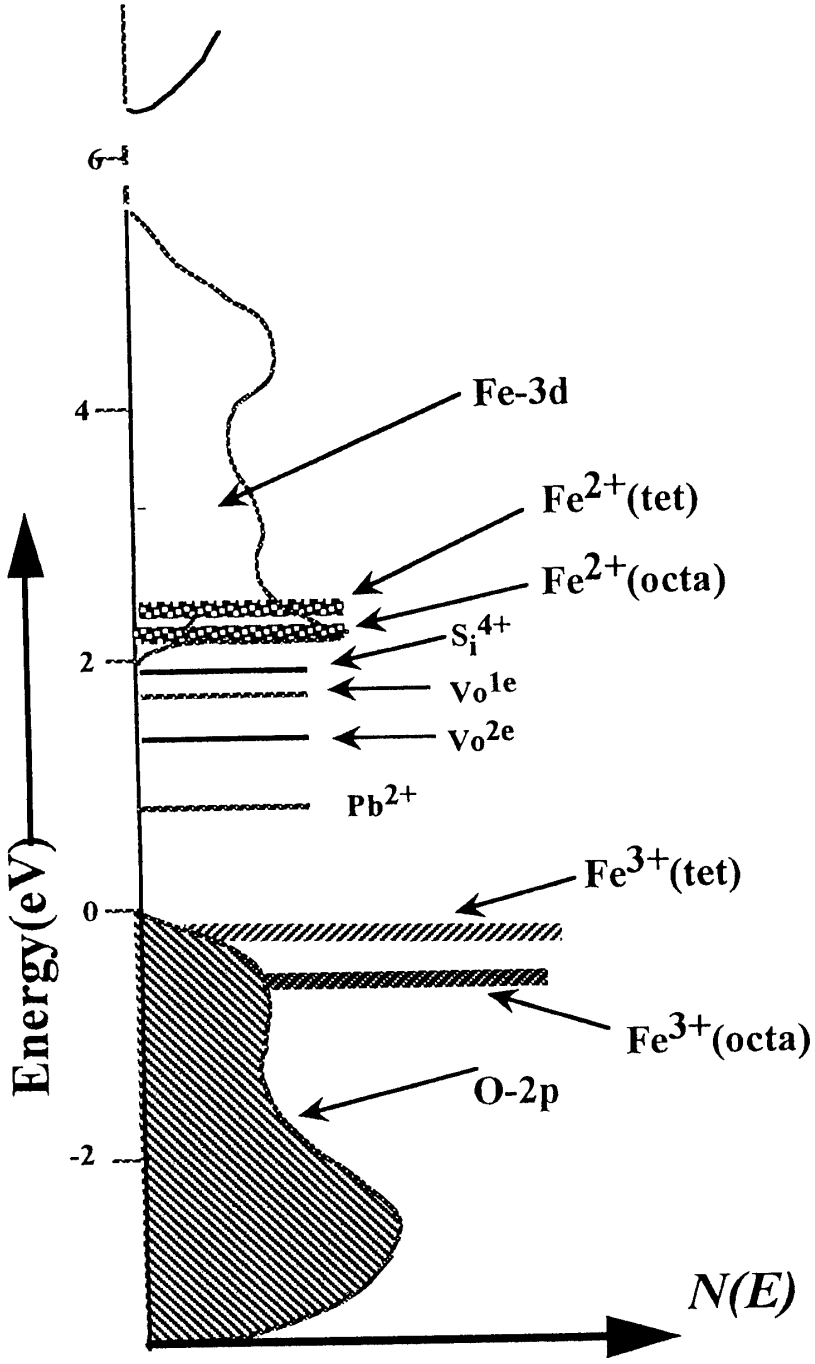

Fig.9 Proposed density of states diagram for yttrium iron garnet (Larsen and Metsellar). Hatched areas denote states filled at T= 0 K. The zero point of the energy scale is set at the top of the valence band.

The observation of a broad structureless band, starting at about 0.6 eV or less, indicates the presence of a broad valence band. In Fig 9, an energy level diagram for YIG may be proposed , based on the information discussed above. The oxygen 2p band (valence band) is a normal one-electron band, which is filled at T= 0 K. The two Pe^{3+} bands form narrow bands due to the localized nature of these states and are also filled at T = 0 K. These two narrow bands have to be situated at a lower energy than the energy level of the Pb acceptor, because otherwise the extra absorption in YIG: Pb cannot be explained. The relative position of the top of the oxygen 2p-band and the Fe^{3+} bands still has to be determined. In Fig. 9, the Fe^{3+} is situated at the top of the oxygen band (which is taken as zero on the energy scale). In accordance with this identification of the conduction band with the lowest $Fe^{3+}(t_{2g})$ level, this level is situated at approximately 2.9 eV, while the Fe^{2+} level is placed near 3.4 eV[30]. We have drawn two broad bands at higher energies denoting the $Fe^{3+}(e_g)$ and $Fe^{2+}(t_{2g})$ levels. These levels probably are the final states for the strong charge transfer transitions which are observed in the absorption spectra above 3.4 eV. Above about 8 eV the broad conduction band formed by metal s-states is drawn. In the energy gap between the valence band and the Fe^{2+}, band some possible donor levels and the Pb acceptor level are shown. The oxygen vacancy Vo is assumed to be deeper donors than Si^{4+}, since we always find a smaller conductivity with a higher activation energy in oxygen deficient than in Si doped YIG. The picture of the donor states given, here is, however, very schematically because donor complexes (donor Fe^{2+}) can also be formed. From the discussion, it will be clear that a further identification of the energy level diagram awaits supplementary experimental data.

4.5 Contribution of vacancy migration to photoinduced DA(PDA)

System of YIG consists of a bound ferrous ion-oxygen vacancy complex having four-fold symmetry and exhibiting a local four-fold symmetry. This is similar to i.e., DX center in Al GaAs. The local anisotropies average to zero when the number of occupied centers is the same. Then, if the distribution is made unequal by illumination, the anisotropy is formed. However, it should be noted that our experiment is not for total anisotropy but for domain wall dynamics. At low temperature, oxygen vacancies Vo behave as a type of charge reservoir which consists of two electrons trapped at the sites (Vo^{2e}) or (Fe^{2+} -Vo- Fe^{2+}) and light sensitive injector of free electrons into this insulating system. That is, the photoexcitation is the alternative method of variation of the free carrier concentration. This process may be illustrated schematically in Fig 10. . These results are interpreted within the context of configuration coordinate(CC) diagrams with large lattice relaxations. In this figure , the point A on the lowest curve corresponds to the total energy in its ground state or (Fe^{2+} -V_o- Fe^{2+}) ; the concave B is (Fe^{2+} -V_o) + Fe^{2+} (nearly free) and the central curve B* is (V_o)+ 2 Fe^{2+} (nearly free) and the upper curve is (Vo) +2Fe^{2+} (free). The direct process begins with electronic excitation by a photon absorbed at Vo^{2e} situated at Q_0 (A → A*) and then through several paths at Q_1 (B →B*). The process of the former (A →A*) needs the much more photon energy than that of the latter (B →B*). So far the discussion is limited to the situation assumed only for electrons or Fe^{2+} but may be extended for holes or Fe^{4+} . In some materials the transport is strongly inhibited by electron-phonon coupling, namely by forming small polarons or self-trapped states. Here the particles are localized and are essentially immobile. The criterion for the self-trapping has been shown to be ELRB, where

ELR is the lattice relaxation energy and B is the band transfer energy. The model of the self-trapped exciton in YIG is unclear but probable future problem. The relative positions of the configuration coordinate parabolas is a crucial parameter, leading to either normal or metastable states. Such states are called large lattice relaxation states and are believed to be responsible for a broad class of metastable phenomena observed in many doped semiconductors. The above discussion is based on the assumption that the strength of defect lattice coupling depends critically on the localization of the electron or hole wave function at the defect. If during any transition this localization changes substantially (e.g. in transition from a localized state to a delocalized defect bound state or in charge transfer involving a localized defect), the lattice around the defects usually undergoes strong rearrangement. The total energy of the system E (electronic and elastic) is plotted versus the local lattice displacement represented by the so-called configuration coordinate Q. A microscopic and quantitative description is quite complicated due to the interference of various interactions among electrons, holes, vacancies and impurities.The microscopic explanation must await detailed analysis of these interactions. Largely overlooked, however, in earlier analysis, we believe the study of these relaxations is helpful for understanding the photomagnetic center in YIG[31-50].

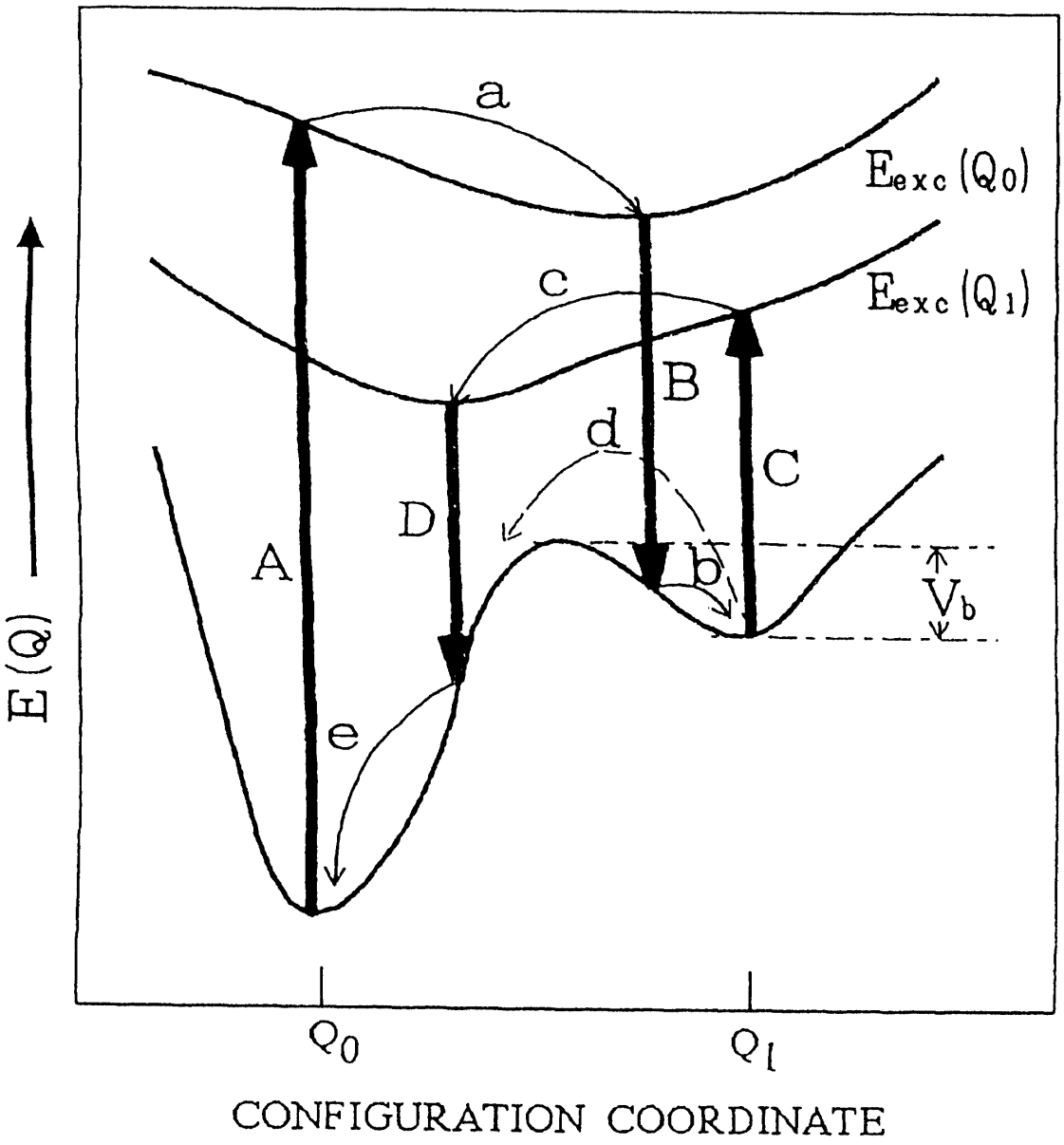

Fig. 10 Configuration coordinate diagram. Arrows with the full lines; photoexcited transition or optical back reaction. Arrows with the dotted lines; thermal transition.

Appendix I

The normalized DA amplitudes of $\mu\_'(t,T)$ measured between t_1 and t_2 is expressed as

$$\Delta\mu'(t_1, t_2, T) = \mu'(t_1, T) - \mu'(t_2, T) \qquad \text{(A1)}$$

and if the simple exponential time dependence is assumed,

$$\Delta\mu'(t_1, t_2, T) = \exp(-t_1/\tau) - \exp(-t_2/\tau) \qquad \text{(A2)},$$

where the relaxation time τ is given by Arrhenius equations $\tau = \tau_0 \exp[Q/kT]$ with the pre-exponential τ_0 and the activation energy Q.
The relaxation time τ at the temperature T_{max} of the DA peak is given by the differentiation of (A2) with respect to T. Thus we have[31]

$$\tau(T_{max}) = (t_2 - t_1)/\ln(t_2/t_1) \qquad \text{(A3)}.$$

The temperature dependence of τ can be determined ,for an example, by a variation of t_2 at the fixed t_1, so the activation energy Q can be obtained.

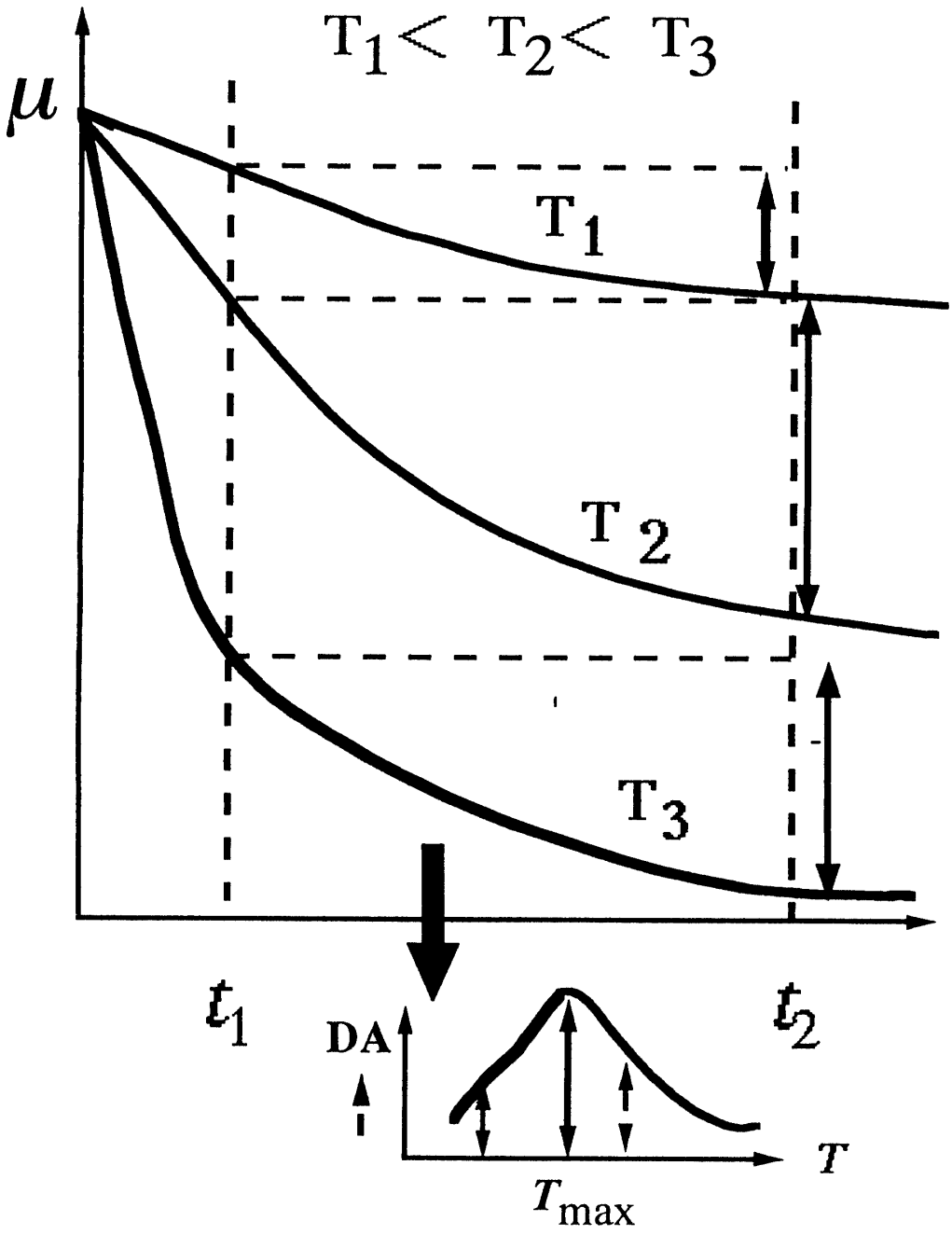

$$\tau_{max}=(t_2-t_1)/\ln(t_2/t_1)$$

$$=\tau_0 \exp(E/kTmax)$$

at the temperature of DA peak, T_{max}

Fig.11 Method of constraction of isothermal relaxation curves from isothermal relaxation curves[3].

Appendix II

This letter is from Professor Dr. Friedlich Walz of Max-Planck-Institute fur Metallforschung Institute fur Physik.(see the text for details).(1997).

MAX-PLANCK-INSTITUT FÜR METALLFORSCHUNG
INSTITUT FÜR PHYSIK

Professor Dr. rer. nat. Friedrich Walz

Prof. Dr. F. Walz, MPI für Metallforschung / Physik
Heisenbergstraße 1, D-70569 Stuttgart

Heisenbergstraße 1
D-70569 Stuttgart

Telefon (07 11) 6 89 - 0
Durchwahl (07 11) 6 89 - 18 17 / 19 11
Telefax (07 11) 6 89 - 10 10

Telex 7 - 255 555

e-mail:
walz@vaxph.mpi-stuttgart.mpg.de

19.9.1996

Prof. Dr. K. Hisatake
Department of Physics
Kanagawa Dental College
Kanagawa 238
- Japan -
FAX-Nr.: (+81) 0468-22-8831

Dear Prof. Hisatake,

As mentioned in the E-mail, we send you with this letter the MAE-spectrum, together with the temperature dependence of the initial susceptibility, obtained on your un-illuminated crystal which, surprisingly, was not influenced at all by the following illumination techniques:

1st Illumination Experiment

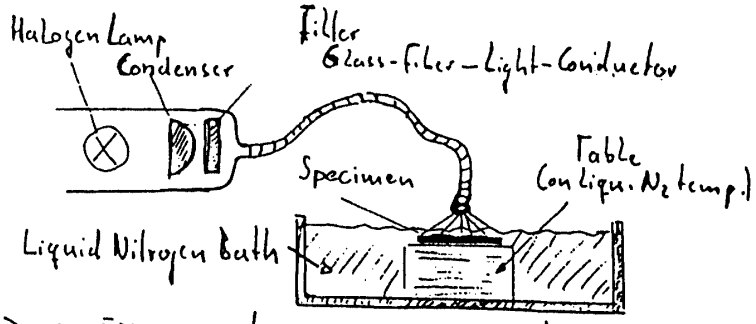

2nd Illumination Experiment

Same mounting as (1), however without the filter!

3rd Illumination Experiment

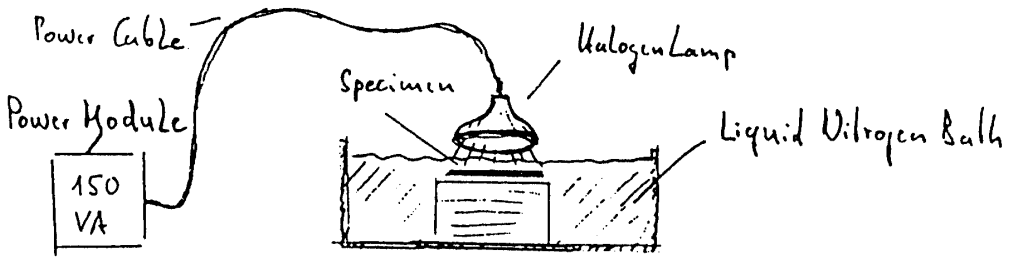

Once more, many thanks in advance for your helpful commemts,

Yours sincerely

Dear Prof. Hisatake,

Since our meeting in Bordeaux, we have made a series of measurements on your crystal but - to say it at the beginning - were not able to reproduce your illumination effect and - even worse - could not detect the least indication of any magneto-optic interaction. Perhaps you may find out from the following description what we have made wrong:

1.) Immediately after cutting the crystal into prismatic form, we obtained - on the un-irradiated sample - a pronounced, interesting MAE spectrum which, however, after a series of modified illumination procedures did not change in the least (a copy of this spectrum is sent to you by FAX):
2.) First illumination was done during 10 minutes by means of a halogen lamp (15 V, 10 A), as used for object illumination in connection with light-microscopes, which allowed perfect focussing of the light-spot on the sample suface, using a glass-fiber optic. During illumination, the sample was in a liquid nitrogen bath, thereby being covered by a layer of about 5 mm. After switching off the lamp, the specimen was mounted, during about 10 minutes - always under liquid nitrogen - into our specimen holder and rapidly cooled down to liquid helium temperature, from which our measurements started and were continued up to about 460 K. The time elapsed during heating up from 4.5 K to 80 K (the temperature at which you usually begin with your measurements) was about 6 hours:
no illumination effect.
3.) After we got aware that this ligh-source contained a filter, reducing the transmitted light to wavelengths below 600 nm, we eliminated this filter for our second illumination experimens (under the conditions of (2.)), still making use, however, of the about 1 m long glass-fiber light conductor:
no illumination effect.
4.) In our third illumination variant, we omitted also the glass-fiber cable and illuminated the specimen directly by means of the lamp, being mounted in a distance of about 20 mm above the surface of the liquid nitrogen (i.e. 25 mm above the sample surface). To our astonishment we didn't obtain, once more, the least illumination effect (illumination time: always 10 min).

After this series of unsuccessful experiments we don't know at the moment how to continue best and therefore ask you if you have an explanation for our failure. What we are asking ourselves:

a) Can you really exclude that your specimen may be optically inactive ?
b) Is it perhaps necessary to prepare the sample surface for effective penetration of the light ?
c) May there exist a time/temperature problem in connection with the times/temperatures quoted under (2.) ?

PLease let us know, which way we should procede to reproduce your most interesting magneto-optical effects. In addition to this E-mail we send you a letter with the MAE spectrum, obtained on your crystal over the temperature range 4.5 K - 460 K, in addition to some sketches illustrating our illumination techniques.

Many thanks in advance for your good advices, with best greetings

Yours Friedrich Walz and Luis Torres.

Prof. Dr. Friedrich Walz
Max-PLanck-Institut fuer Metallforschung
Institut fuer Physik
Heisenbergstr.1
D-70569 Stuttgart / Germany

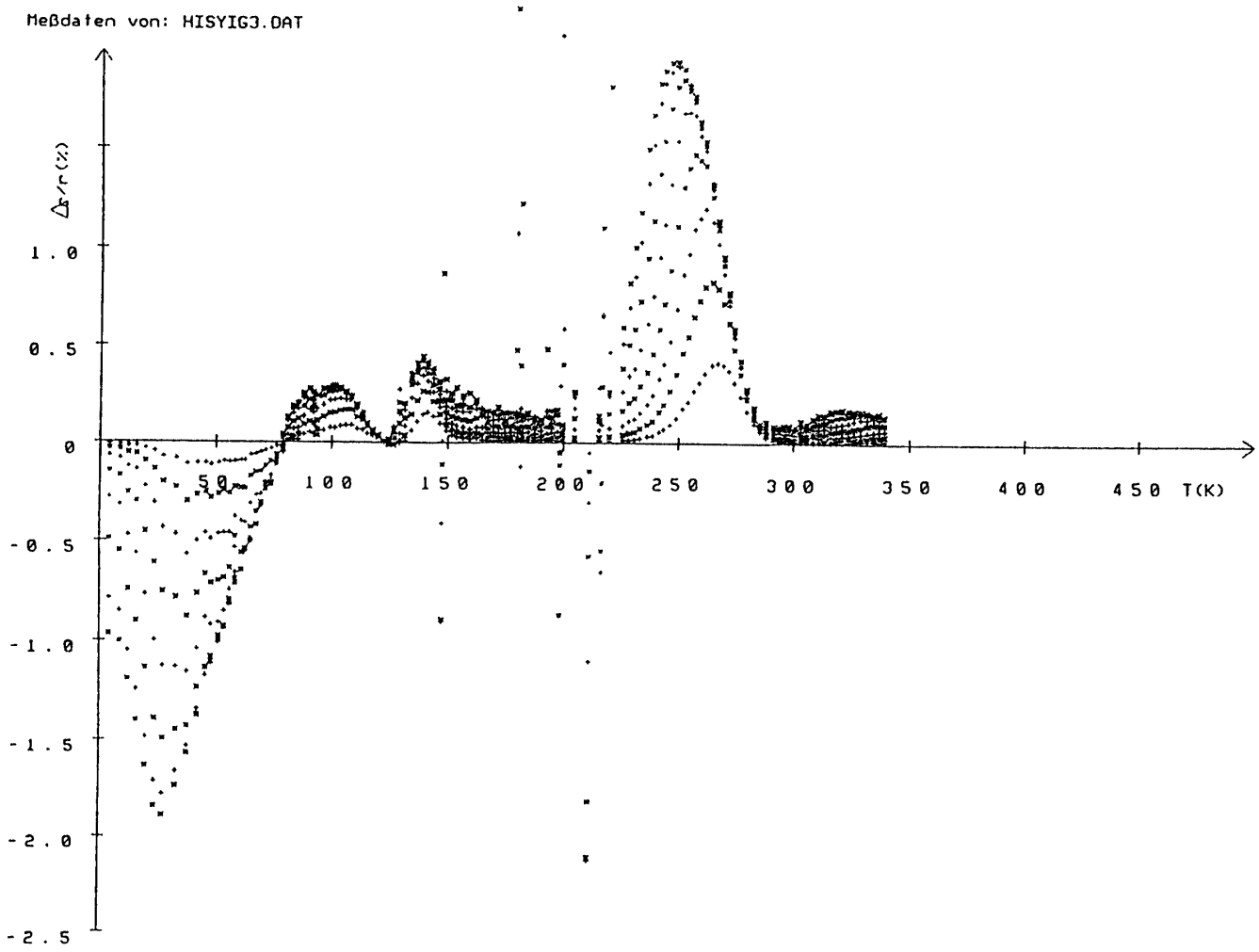

Fig.12 Experimental results by F.Walz.(No1)

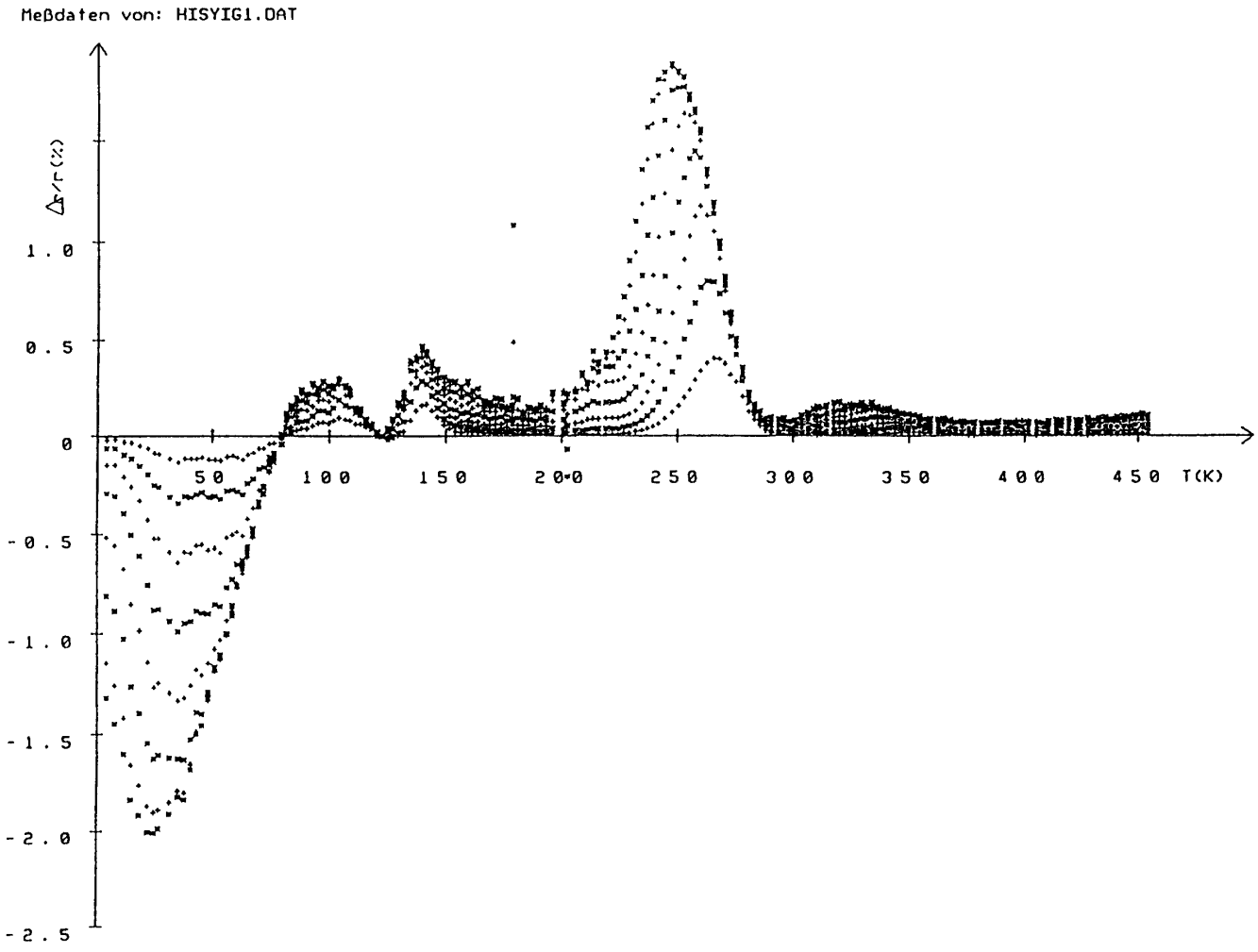

Fig.14 Experimental results by F.Walz.(No.3)

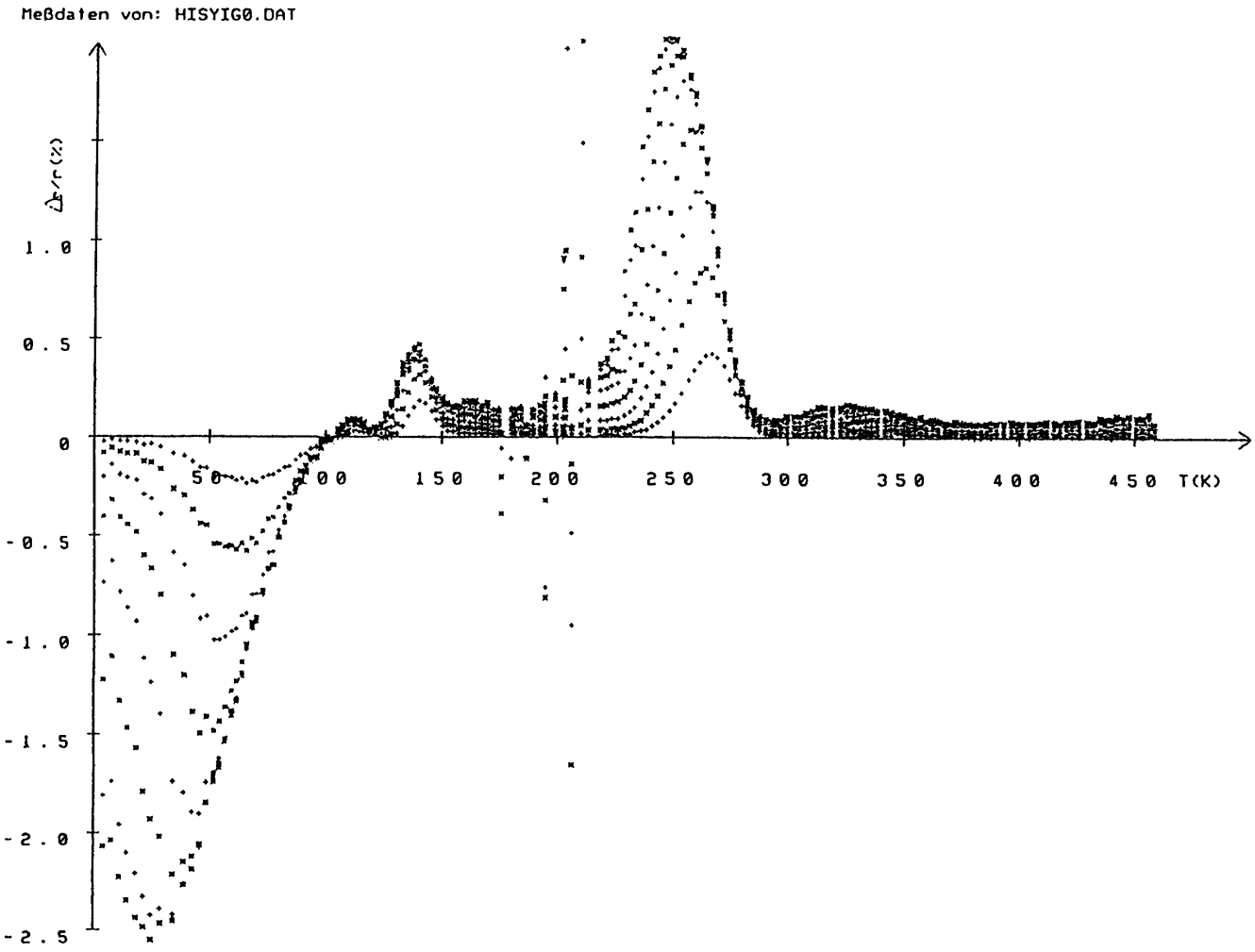

Fig.14 Experimental results by F.Walz.(No.3)

References

1)Alejos, C. de Francisco, P. Hernadez, K. Bendimya, and J. M. Munoz,
Appl. Phys. A: Mater. Sci. Process. 63A, 471 (I 996) .

2) C. de Francisco, J. Eiguez, and J. M. Munoz, An. Fis. Ser. B 81, 271 (1985).

3)H.Kronmüller, Vacancies and Interstitials in Metals(North-Holland,Amsterdam,1969) 667.

4)H.Kronmller, Nachwirkung in Ferromagnetika (Springer-Verlag, Berlin, 1968). 12

5)L.Torres, C. de Francisco, L. Torres, R. de Miguel, P. Hernandez, and J. I. iguez, J. Phys. IV 7, Cl-289 (1997).

6)M. Guyot, T. Merceron, and V. Cagan, J. Phys. D 16, L93 (1983).

7) S. Chikazumi. Physics of Magnetism (Wiley, New York, 1964). 21.

8)L. Snoek, Physica (Amsterdam) 5, 663 (1938).

9) L. Neel, J. Phys. Radium 13, 249 (1952).

10)S. Krupicka and K. Zaveta, Anisotropy, Induced Anisotropy and Related Phenomena (Wiley, New York, 1975).

11) G. H. J. Wantenaar, G. V. Wilson, D. H. Chaplin, and S. J. Campbell, J. Magn. Magn. Mater. 89, 13 (1990).

12)K. L. Ngai, Comments Solid State Phys. 9, 141 (1980).

13) U. Enz, R. Metselaar and P.J.Rijnierse,*J. Phys.*,**32C**1,702(1971).

14) S. Chikazumi , Physics of Ferromagnetism, (Clarendon, Oxford, 1997).

15) K.Hisatake, I. Matsubara, K.Maeda, T. and Y.Kawai and S.N.Lyakhimets, **IEEE** Trans.,**30** 975(1994).

16) Private communication: Prof. S.Kurita of Yokohama National University.

17) K.Hisatake, I. Matsubara, K.Maeda, and K.Uematsu, *J.Mag.Mag.Mat.*,**112**, 385(1992).

18)K.Hisatake, I. Matsubara, K.Maeda,Proc.ICF **VI** ,749(1992).

19) S.N. Lyakhimets and V.F.Kovalenko, Ukrain.Fiz.Zh.,**30** ,1522(1985).

20) O. Alejos, C.de Francisco, J. M. Munoz, P. Hernandez, and C. Torres, Phys. Rev., **B58**. 8640(1998).

21) H.Kronmüller, Vacancies and Interstitials in Metals(North-Holland,Amsterdam,1969) 667.

22) I.Matsubara, Doctor Thesis (1999, Tohoku University)

23)U. Enz, R. Metselaar and P.J. Rijnierse, ***J.Phys.* 32 C1** 702(1971).

24)S. Chikazumi , Physics of Ferromagnetism, p.537(Clarendon, Oxford, 1997).

25)K.Hisatake, I. Matsubara, K.Maeda, and Y.Kawai and S.N.Lyakhimets, **IEEE** Trans., **30** 975(1994).

26)R.E.Fontana and D.J.Epstein, Mater.Res.Bull.**6**,959(1971).

27)O.Alejos, C.de Francisco,J.M.Munoz,P.Hernandez, and C. Torres, Phys. Rev. **B58**. 8640(1998).

28) R. Metselaar and P.K. Larsen, Solid State Comm. **15**, 291 (1974).

29)P. K. Larsen and J. Robertson, J. Appl. Phys. **45**, 2867 (1974).

30) R. Metselaar, J. Phys. Chem. Solids **34**, 2257 (1973).

31)K.Hisatake.,I.Matsubara.,K.Maeda: Joural de Physique IV**8**(1998)367.

32)K.Hisatake.,I.Matsubara, K.Maeda:Journal of the Magnetics Society of Japan Vol.**22**(1998) 49.

33)S.Kainuma and K,Hisatake Journal of the The Magnetics Society of Japan Vol.**21**(1998)224.

34)S.Kaimuma and K.Hisatake, Journal of The Magnetics Society of Japan Vol.**21**(1997) 557.

35)Title of the book:. **SERGEY .N. LYAKHIMETS**
S. N..Lyakhimets and K.Hisatake: Band Model of Photoinduced Magnetic Effects in YIG:Si(p.224-227).
K.Hisatake ., I.Matsubara., K.Maeda and S.N Lyakhimets. ·· Photoinduced Irreversible and Reversible Magnetic Permeability in Yttrium Iron Garnet(pp.228-239). ;Irreversible and Reversible Phenomena in Yttrium Iron Garnet (pp.259-261) .; Photoinduced Disaccommodation in Oxygen Deficient YIG, Printed ··National Academy of Sciences and Ministry of Education of Ukraine Institute of Magnetism, 1997.
36)S.Kainuma, and K.Hisatake, Research Report of Ashikaga Institute of Technology **22** 77 (1996).
37) K.Hisatake ., I.Matsubara., K.Maeda ··Bulletin of Liberal Arts and Sciences(KDC)**15**,58,1997.
38)K.Hisatake ., I.Matsubara., K.Maeda ·· Journal of Magnetic Society of Japan **21**, 629, 1997.
39)K.Hisatake ., I.Matsubara., K.Maeda ··Bulletin of Liberal Arts and Sciences, Kanagawa Dental College, **14** : (1996) 48.
40) K.Hisatake, I.Matsubara, . K. Maeda: J.Magne. Magne.Mater.**143** (1995)2127.
41) K.Hisatake, I.Matsubara, K.Maeda: Proc. IUMRS-ICE'94 Vol.**3** (publ. 1995)139.
42)K.Hisatake, I.Matsubara, K.Maeda: IEEE Trans. on Magnetics (American Inst.ele.electronics engineering)34(1995)826; Jornal of Magnetism ,Magnetic Materials(Amsterdam)144(1995)2127.
43) K.Maeda,I.Matsubara,K.Hisatake: J . of Magnetic Society of Japan **15**(1991)201.
44)K.Maeda and K.Sato, Physica B(Amsterdam)**226**(1995)451.
45) K.Hisatake, I.Matsubara, K.Maeda, Journal of Fabrication and Characterization of Advanced Materials **I** (1995)139.
46) K.Hisatake, I.Matsubara, K.Maeda, Materials Chemistry and Physics'Elsevier) **43** (1995) 1689.
47)I.Matsubara K.Maeda and K.Hisatake: **IEEE** Trans. on MAGNETICS (American Inst. Elect. Electron.Eng.) **30** (1994) 975.
48) K.Hisatake,I.Matsubara,K.Maeda,Y .Kawai and K.Uematsu, Proc.2nd Int. Symp. Phys. of Magnetic Materials,(Beijing China), 546 (1992).
49) K.Hisatake, I. Matsubara,K.Maeda, Proc. of Inter Conf .of Ferrites **VI** 749 (I 992 ,Tokyo).
50) H.Yasuoka, H.Mazaki, K.Hisatake, I. Matsubara, K.Maeda, K.Uematsu, Materials Chemistry and Physics, **45** 71 (1996).